Journal of Alloys and Compounds, 211/212 (1994) 245–248
JALCOM 016

Measurement of hydrogen solubility during isothermal charging in a Zr alloy using an internal friction technique

Z.L. Pan, M.P. Puls and I.G. Ritchie
Materials and Mechanics Branch, AECL Research, Whiteshell Laboratories, Pinawa, Manitoba ROE 1L0 (Canada)

Abstract

A proportionality between Young's modulus and the hydrogen concentration in solid solution of alloys of Zr has been reconfirmed. This proportionality is used to monitor the increase in hydrogen content during isothermal hydrogen charging.

1. Introduction

The presence of hydrogen in zirconium alloys can result in severe embrittlement, because brittle Zr hydrides and/or deuterides are precipitated when the terminal solid solubility (TSS) of hydrogen is exceeded. For nuclear engineering applications, a knowledge of the TSS of hydrogen in Zr alloys is crucial to assess the potential for delayed hydride cracking [1]. Several techniques have been used to determine the TSS [2–4]. Of these, internal friction has been shown to be a very powerful technique for the study of hydrogen in metals. Cannelli and Mazzolai [5] demonstrated that an internal friction peak can be used to detect the onset of hydride precipitation sensitively and to determine the TSS in hydride-forming metals. The Zr–H system has been extensively investigated using this technique [6–13] yielding a temperature spectrum of internal friction peaks.

At low frequency (~ 1 Hz), the spectrum can be split into two parts. The first part consists of three relaxation peaks, labelled P_1, P_2 and P_3. These are attributed to lattice dislocation relaxation and the stress-induced growth/shrinkage of γ- and δ-hydride precipitates, respectively. The second part consists of a truncated peak, which appears at the TSS temperature of the specimen. During heating the peak is associated with hydride dissolution and is truncated more or less sharply at TSSD, the dissolution TSS. During cooling the peak is associated with hydride precipitation and growth and is very sharply truncated at TSSP, the precipitation TSS. Both peaks are accompanied by a "knee" in the corresponding dynamic elastic modulus curves. In some commercial Zr alloys, the precipitation/dissolution peaks are absent even at low frequency and high heating or cooling rate that are known to increase the peak height in pure Zr, but the knee point in the curve of modulus *vs.* temperature is always observed and is a physical marker of the TSS [9, 13].

Theoretical models of TSS and hydrogen supersaturation in hydride-forming metals have been proposed by Puls [14, 15]. It is expected that a clearer knowledge of the TSS will be achieved by combining the results of internal friction experiments with the theoretical studies. The purpose of this paper is to extend the internal friction technique to the study of the isothermal ingress of hydrogen into an experimental, Zr-based pressure tube alloy.

2. Experimental details

Measurements of internal friction (Q^{-1}) and Young's modulus (E) at frequencies of 40 kHz and 120 kHz had previously been carried out with an automatic piezoelectric ultrasonic composite oscillator technique (APUCOT) operated in the longitudinal vibration mode at a constant strain amplitude $\sim 2\times 10^{-7}$. Details of the technique are given elsewhere [16]. A precision of $\sim 1\%$ in Q^{-1} and of $\sim 0.01\%$ in E can be obtained using the APUCOT. Two types of tests were carried out in the following. In the first type, the test procedure consisted of thermally cycling a specimen at a constant heating and cooling rate through the TSS temperature. During the thermal cycles Q^{-1} and E were continuously measured using the APUCOT and the TSS temperature obtained from the "knee" in the curve of E *vs.* T. An equation of the TSS boundary was obtained by measurement of the TSS temperature on a set of specimens containing different hydrogen concentrations as demonstrated in Fig. 1.

Elsevier Science S.A.
SSDI 0925-8388(93)00016-R

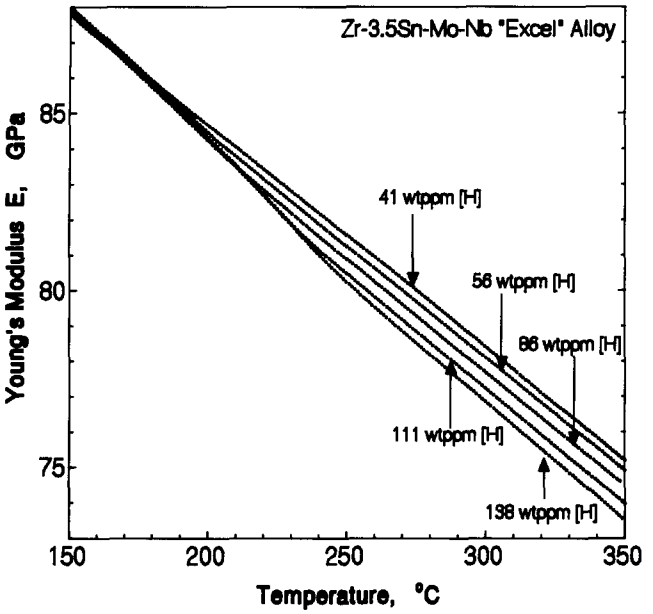

Fig. 1. Plots of Young's modulus *vs.* temperature for Excel containing different levels of H.

In the second type of tests, the information obtained in the first type was used to study the process of hydrogen charging. A mixture of $Ar+1\%H_2$ gas was passed through the heating chamber at a constant rate. The specimen tested was maintained at 250 °C with a stability of ± 0.1 °C, while Q^{-1} and E were continuously measured as a function of time during the isothermal charging.

The specimens used for both types of tests, of dimensions $3\times3\times48$ mm^3, were cut from the longitudinal direction of a section of an experimental pressure tube. The composition of the experimental Zr alloy, Excel, is 3.5% Sn, 1% Mo, 1% Nb with the balance Zr (all wt.%). The Zr alloy consists predominantly of elongated, α-phase, hexagonal-close-packed grains, surrounded by a continuous grain boundary network of β-phase. Each specimen tested was coated with a very thin layer of Ni to increase the rate of hydrogen charging.

3. Results and discussion

3.1. Young's modulus measurement

Young's modulus as a function of temperature was measured on several specimens containing different levels of hydrogen. Some curves of E *vs.* T during cooling are shown in Fig. 1. When the temperature is higher than the TSS temperature, all of the hydrogen atoms are in solid solution. In this temperature range, a linear relationship between E and T is observed. An equation of the form $E=E_0+A\cdot T$ for each specimen can be obtained by linear regression. The proportionality between Young's modulus and the hydrogen concentration may vary with the specimens's microstructure. To ensure that the microstructure did not change and, therefore, that the same linear relationship between Young's modulus and the hydrogen concentration holds for each specimen, identical hydriding treatments and thermal cycles were applied to each specimen.

It is evident from Fig. 1 that Young's modulus in the Zr alloy is depressed by the presence of hydrogen in solution. Also from Fig. 1, it can be shown that the depression of Young's modulus is proportional to the hydrogen concentration (C_H) in solution, so that plotting E *vs.* C_H yields the linear relationship shown in Fig. 2. Two mechanisms have been suggested [13] to explain this effect. The first mechanism is a direct effect of the hydrogen atoms on the stiffness of the Zr lattice through a change of the interaction forces between neighbouring Zr atoms. The second attributes the depression of E by hydrogen in solution to one or more modulus defect effects due to anelastic relaxation involving hydrogen in solution (*e.g.* a hydrogen Snoek–Koster peak) at low temperatures. In either mechanism, the reduction of the elastic modulus must be proportional to the hydrogen content, at least in the case of dilute Zr–H alloys, in order to account for the observed results.

The linear relationship between E and C_H can be used to monitor the variation of C_H, during hydrogen ingress, by continuously determining E during any hydrogen charging process. In this paper, it is employed to detect the onset of the nucleation of hydrides during isothermal hydrogen charging, as described below.

3.2. Hydrogen charging

Young's modulus as a function of hydrogen charging time at 250 °C in as-received Excel specimen was

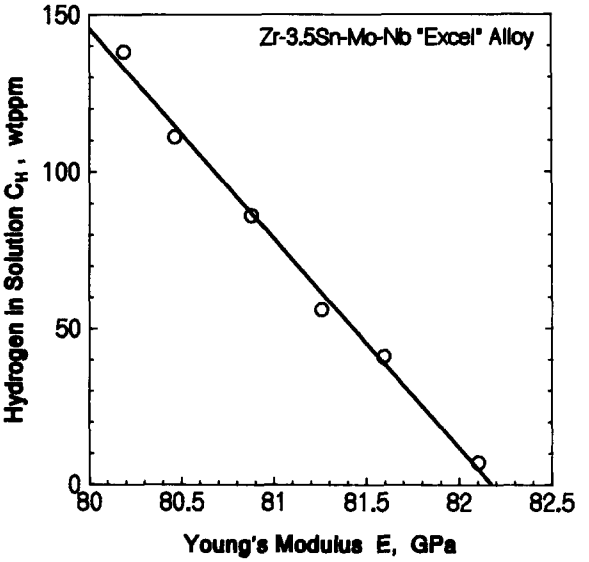

Fig. 2. A linear relationship between Young's modulus at 250 °C and hydrogen content in solution for dilute Zr–H Excel alloy.

continuously measured. Using the linear relationship between C_H and E (Fig. 2), the hydrogen concentration in solution as a function of charging time can be calculated and is shown in Fig. 3. The estimated error for the measurement of the hydrogen content in solution is within ± 5 wt.p.p.m. After each hydrogen charging period, two thermal cycles at a rate of 1 °C min^{-1} between 250 °C and 24 °C were conducted while Q^{-1} and E were measured continuously. The results of this thermal cycling are discussed in the next section.

During the first period of charging, the hydrogen content apparently became supersaturated, (with respect to the dissolution TSS (TSSD)) causing initiation of hydride nucleation on the 18th day (430 h), at a level of 105 wt.p.p.m. After this, C_H remained approximately constant with fluctuations of ± 5 wt.p.p.m. for more than 48 h. During the second period, hydride precipitation occurred on the 21st day (500 h) at a level of 110 wt.p.p.m. During the 3rd period, precipitation did not occur until the 25th day (600 h), at a level of 105 wt.p.p.m., while during the 4th period, precipitation did not occur until the 28th day (680 h). For the 1st, 2nd and 3rd periods, the concentration of hydrogen in solution was close to 110 wt.p.p.m. when precipitation occurred. This concentration level is temporarily designated as the "isothermal TSS" (TSSI). In this Zr alloy at 250 °C, the precipitation TSS (TSSP) and the dissolution TSS (TSSD) were calculated from the equation for the solvus to be 123 wt.p.p.m. and 60 wt.p.p.m., respectively. It is seen that TSSI is close to, but measurably less than, TSSP and considerably higher than TSSD. This implies that the hydrogen picked up by a Zr alloy pressure tube during reactor operation is only precipitated as hydride when the hydrogen concentration approaches TSSP (cool-down) rather than TSSD (heat-up). The above results are significant in that they confirm the postulated role that the hysteresis in the TSS plays in causing hydrogen supercharging in Zr alloy specimens under suitable hydrogen charging conditions [15]. It should be noted that the above solubilities for Excel are considerably higher than corresponding ones for Zr or its alloys such as the Zircaloys and Zr–2.5Nb. The reason for this higher solubility has not been established, but may be associated with the greater proportion of β-phase in Excel.

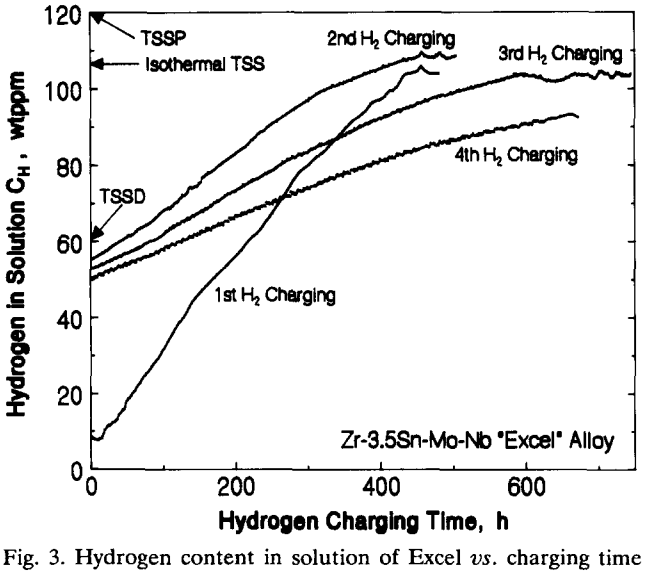

Fig. 3. Hydrogen content in solution of Excel *vs.* charging time at 250 °C for four consecutive periods of hydrogen charging.

3.3. Thermal cycle effect

Starting with a specimen of Excel containing a typical, as-received, amount of hydrogen (<10 wt.p.p.m.), the hydrogen in solution was completely supersaturated at a level of 105 wt.p.p.m. at the end of the first period with newly ingressing hydrogen atoms being precipitated. After two thermal cycles, at the beginning of the second period, the starting hydrogen content in solution was about 50 wt.p.p.m., with the remaining 55 wt.p.p.m. of hydrogen atoms, collected during the first charging period, contained in the hydrides. During the second period, despite the presence of hydrides, the newly ingressing hydrogen atoms stayed in solid solution until the hydrogen content in solution arrived again at the supersaturation level of about 110 wt.p.p.m. This implies that during the second charging period the amount of existing hydride remained at a constant level until complete supersaturation of hydrogen in solution had occurred. A similar phenomenon was observed for the third and fourth charging periods. Average rates of hydrogen charging were estimated to be 5.8, 3.3, 2.6 and 1.9 wt.p.p.m. day^{-1} for the first, second, third and fourth periods, respectively. One possible reason for this trend of decreasing rate is that beyond 110 wt.p.p.m., the newly ingressing hydrogen atoms had accumulated in surface hydrides layers and the hydride-rich layers slowed the consequent ingress. Another possibility is that the oxidation of the specimen's surface during the long-term tests formed a barrier to hydrogen ingress. We expect that a decreasing ingress rate would favour a more uniform distribution of hydrides and reduce the tendency for hydride layering near the surface.

3.4. P_2 peak

During the thermal cycles, an internal friction peak at 80 °C was observed with a frequency of 40.573 kHz. The peak height increased with the amount of hydride present, as shown in Fig. 4. The peak appears to be the P_2 peak previously reported [5–8, 11, 12]. However, the P_2 peak measured in Excel Zr alloy is wider than that observed in pure Zr and Ti. At the APUCOT second overtone of 121 kHz, the P_2 peak was only detected in specimens containing more than 300

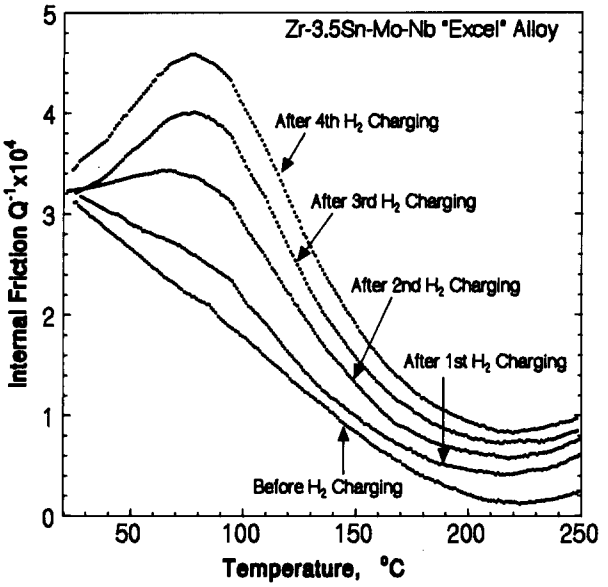

Fig. 4. P_2 peaks as a function of hydrogen charging.

wt.p.p.m. hydrogen. The P_2 peak has been attributed to the stress-induced growth/shrinkage of the metastable γ-hydride [12]. To date, a resolved P_3 peak has not been detected in this material. However, in this alloy P_2 and P_3 might overlap considerably giving rise to the broad peak observed.

4. Conclusion

A linear relationship between Young's modulus and the hydrogen concentration in solution for dilute Zr-based alloys at a given temperature has been confirmed and quantified for the experimental pressure tube alloy, Excel. The proportionality between the depression of Young's modulus and hydrogen concentration in solution was used to monitor the variation of hydrogen in solution during hydrogen charging. Hydride nucleation during such an isothermal hydrogen charging process was detected by this technique. The results show that the hydrogen picked up by an alloy of Zr precipitates as hydride only when the hydrogen content is close to, but less than the TSS for precipitation (TSSP).

Acknowledgment

This work was funded by the CANDU Owners Group (COG) under WPIR 2-31-6580.

References

1 R. Dutton, *Met. Soc. CIM Annual Volume, 16* (1978) 16–25.
2 J.J. Kearns, *J. Nucl. Mater., 22* (1967) 292–303.
3 A. Sawatzky and B.J.S. Wilkins, *J. Nucl. Mater., 22* (1967) 304–310.
4 C.E. Coleman and J.F.R. Amber, *Met. Soc. CIM Annual Volume, 16* (1978) 81.
5 G. Cannelli and F.M. Mazzolai, *Nuovo Cimento, B64* (1969) 171.
6 F. Povolo and E.A. Bisogni, *J. Nucl. Mater., 29* (1969) 82–102.
7 V. Provenzano, P. Schiller and A. Schneiders, *J. Nucl. Mater., 52* (1974) 75–84.
8 F.M. Mazzolai, J. Ryll-Nardzewski and C.J. Spears, *Nuovo Cimento, 33 B* (1976) 251–263.
9 K. Nuttall, R. Dutton and A.J. Shillinglaw, *Hydrogène et Matériaux Congres International, 3ème,* Paris, 1982, Vol. 1, 167–172.
10 I.G. Ritchie and K.W. Sprungmann, *J. de Phys., 44* (1983) C9-313-318.
11 H. Numakura, T. Ito and M. Koiwa, *J. Less-Common Met., 141* (1988) 285.
12 I.G. Ritchie and Z.L. Pan, *Phil. Mag., A63* (5) (1991) 1105–1113.
13 I.G. Ritchie and Z.L. Pan, ASTM STP No. 1169 (1992) 385–395.
14 M.P. Puls, *Acta Metall., 32* (1984) 1259.
15 M.P. Puls, *J. Nucl. Mater., 165* (1989) 128.
16 I.G. Ritchie, Z.L. Pan, K.W. Sprungmann, H.K. Schmidt and R. Dutton, *Can. Metall., Q. 26* (1987) 239–250.